

Acetone Chemistry On Oxidized Rutile TiO₂(110)

Patrick Murray,^{*,†} Yaobiao Xia,[‡] Zhenrong Zhang,[‡] Ken Park,[‡] and Ke Zhu[‡]

CASPER NSF Fellow, Baylor University, and Department of Physics, Baylor University

E-mail: pcmurra1@asu.edu

Abstract

Surface defects are known to dominate both the electronic and chemical properties of metal oxide surfaces, an object of much study for use in catalytic processes. In order to study surface chemistry in detail, an ultra-high vacuum (UHV) chamber was designed to combine a LEED and STM system. Construction is underway, with a reported initial base pressure of 10^{-9} Torr revealing no major leaks. On a fully functioning system, we studied the relationship between acetone and oxygen adatoms on rutile TiO₂(110) using scanning tunneling microscopy (STM). We report an acetone-assisted oxygen adatom diffusion mechanism. The STM images from the same area reveal that acetone molecules preferentially adsorb to oxygen vacancy sites at room temperature. Sequences of isothermal STM images directly show that diffusion of acetone over oxygen adatom sites causes apparent motion of the adatoms. We propose a mechanism whereby the acetone diffuses along the Ti_{5c} row and exchanges oxygen with the adatom, creating an apparent motion of the defect.

Introduction

The understanding of point defects is essential to the understanding of the physics and chemistry on the surface of metal oxides. In heterogeneous catalysis between gaseous reagents and a solid catalyst, the adsorption and subsequent dissociation of the molecules usually occurs at surface defect

sites. Defects change the electron configuration of the surface, altering the reactivity of the surface.¹⁻³ The diffusion of molecules on the surface is a key step in most surface mediated reactions. Oxygen is one of the main oxidizing reagents, as many catalytic reactions rely on the equilibrium between the addition and removal of oxygen atoms attached to the surface.

TiO₂ is an important metal oxide used in catalysis, solar cells, gas sensors, pigment, and corrosion-protective coating, among other things.¹ Due to its widespread use, it has been thoroughly studied and become regarded as a general model for metal oxide surfaces. The rutile (110) surface of titania is the most stable and well characterized surface, making it ideal for surface chemistry research. The effect of surface defects on the adsorption and following dissociation of various adsorbates on this surface has been extensively studied.^{1,4,5} It is established that the prevalent surface defect of the vacancy of a bridge-bonded oxygen site (V_O) facilitates the adsorption and subsequent dissociation of water and various alcohols.^{3,6,7} More recently, it has been observed that Ti interstitials below the surface also play a role in the surface chemistry of TiO₂(110).⁸

This study examines the simplest ketone, acetone ((CH₃)₂CO), to study the effects ketones can play on surface defects and how these defects can affect the adsorption of the molecule. Acetone represents not only a common reactant, intermediate, and product in many organic catalytic reactions, but is also commonly present as a contaminant in the air. The acetone interaction with surface defects has been studied before, with our group, Xia and co-workers, reporting on the acetone-mediated diffusion of bridging bonded oxygen va-

^{*}To whom correspondence should be addressed

[†]Arizona State University

[‡]Baylor University

cancy sites, V_O . They report that adsorbed acetone on vacancy sites react with adjacent O_b atoms, leading to the formation of a η^2 -diolate diffusion intermediate. The alkyl group can then move to the next O_b atom via creation of a carbonyl bond. During this process, acetone loses its oxygen and heals the vacancy. This alkyl group can then pick up any O_b atom and migrate to the Ti_{5c} row as a acetone molecule, taking its oxygen with it and creating a new vacancy, leading to the diffusion of the original vacancy.⁹ The purpose of this study is to further research acetone's interaction with point defects by focusing on its interaction with O_a on the rutile $TiO_2(110)$ surface.

In order to obtain a molecular-level visual representation of surface reaction processes, we employed the variable temperature scanning tunneling microscope (STM) to study the surface reaction. Before using an STM to study surface science at the molecular level, however, the proper environment must be created. Under normal conditions, there are about 2×10^{25} molecules/ m^3 in the air, traveling with a mean velocity of around 500 m/s. This causes numerous collisions of gas molecules with the surface of a solid, leading to a high number of adsorbates and reactions on the surface. To adequately compare theory to experiment, and to limit observations to those events caused by the surface's specific chemistry, these side reactions must be minimized. To this end, a UHV (ultra-high vacuum) system is typically employed. UHV systems reach pressures below 1×10^{-9} Torr.

LEED/STM Chamber

Chamber Design and Construction

In order to obtain detailed information about both the surface and structure of TiO_2 and other materials, we designed and began construction on a UHV system to house a low energy electron diffraction (LEED) system and RHK STM together. While the STM gains information only about the surface structure, the LEED provides insights below the surface, detecting the atomic structure through comparison to simulations. It was decided to separate the two systems into a preparation cham-

ber and a STM chamber, as seen in Figure 1. The preparation chamber contains the load-lock, LEED, ion and electron guns. Care was taken to position the LEED out of the line of Ar ions used when sputtering. In this chamber, we can load the sample, then clean it through annealing or sputtering, before analyzing it for its cleanliness and structure with LEED. A bellows, yet to be installed, will connect the two chambers. As the RHK sample holder was not compatible with the one for the LEED, a system of movable arms was designed to transfer the sample from the LEED to the load lock holder, through the bellows to the STM. The entire system rests on an air-lag table to isolate the STM from mechanical vibrations. The LEED, ion gun, and other ports on the preparation chamber have been installed, and the ion and turbo pumps have been connected.

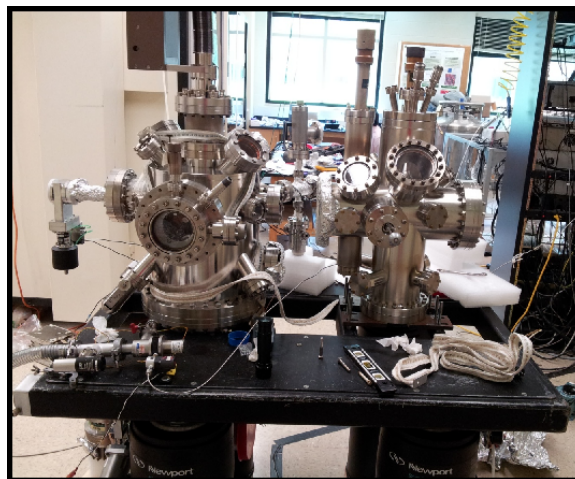


Figure 1: Chamber on left is the preparation chamber, housing the LEED and ion gun. Chamber on right is the STM chamber.

Chamber Testing and Results

After fully connecting the preparation chamber, we surrounded the chamber and ion pump in heating tape and Al foil for insulation and baked the chamber at $160^\circ C$ for one day. After degassing the ion pump, the chamber was pumped for a day, reaching the mid 10^{-9} Torr range. This is in the high-vacuum range, and approaching that of ultra-high-vacuum. This indicates that the chamber is free of any major leaks, and provides an optimistic view for the future of the chamber.

Brief Explanation of STM

The basis behind a Scanning Tunneling Microscope (STM) is based on the concept of quantum tunneling. It consists of an atomically sharp tip over the surface to be studied. A bias is then induced between the sample and the tip, allowing electrons to tunnel from the tip to the sample (positive bias) or from the sample to the tip (negative bias).¹⁰ This tunneling current is approximated by the following relation, where I_t is the tunneling current, E is the energy of the electrons, and κ is a constant related to the applied bias. Z is the distance from the sample to the tip.

$$I_t \propto \rho_s(Z, E)e^{-2\kappa Z} \quad (1)$$

Here, $\rho_s(Z, E)$ refers to the local density of states, as tunneling requires an empty level on the sample/tip of the same energy as the electron attempting to tunnel. Due to the exponential dependence of the tunneling current to position, very small changes in distance between the tip and sample can be observed as measurable changes in tunneling current, allowing the topography of the surface to be inferred from I_t . In reality, however, as the local density of states differs near different elements and molecules, an STM scan of a non-homogeneous surface reveals a convolution of the electronic structure and topography of the surface.

As the new system is not yet operational, the experiment and all images were taken on the system described in the following section.

Experimental Section

The STM experiments were conducted in an UHV system (base pressure 2×10^{-11} Torr) equipped with a variable-temperature STM (SPECS), a mass spectrometer (SPECS), and ion gun (MKS). The single-crystal rutile $\text{TiO}_2(110)$ surface (Princeton Scientific) was cleaned by repeated cycles of Ar ion sputtering at 2 keV and UHV annealing from 800-900 K, with the sample's cleanliness determined by STM imaging. Special care was taken to minimize background water contamination, including baking the chamber to 160°C. At the start of each experiment, the sample was flashed to 600 K to evaporate off water adsorbed from back-

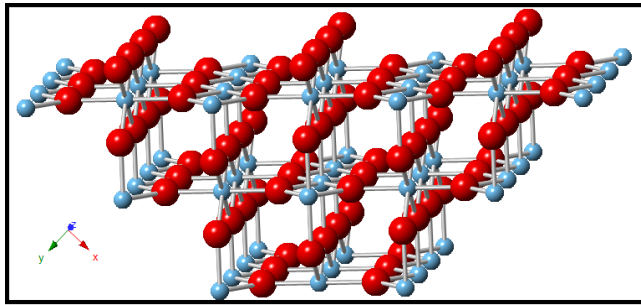


Figure 2: Ball-and-stick model of the (110) surface of rutile TiO_2 . Titanium (blue) atoms are 6-fold-coordinated in the bulk, with surface atoms having 5-fold coordination. Oxygen (red) atoms possess 3-fold coordination in general, with bridge-bonded oxygen (O_b) having 2-fold coordination.

ground molecules. The initial stages of oxygen adsorption were studied by introducing oxygen through backfilling, with experiments carried out at 300 K and 100 K. We analyzed the same areas of the surface before and after oxygen exposure to monitor changes in point defects caused by adsorption of individual molecules. After exposure to oxygen, acetone was allowed to adsorb, with the same surface area being analyzed before and after adsorption in order to monitor how defect concentration and configuration affects acetone adsorption. Acetone was introduced using a directional doser which releases acetone 3 mm from the sample. The STM tip was etched tungsten and prepared by Ar sputtering. STM images presented were collected in constant current (.1 nA) mode at positive sample bias voltage of 0.9 - 1.5 V.

Results and Discussion

Figure 3 shows a typical STM image of a $\text{TiO}_2(110)$ surface at 300 K after exposure to oxygen. In these images, the low, five-fold-coordinated Ti^{4+} ions are imaged as high hills, while the rows of bridging oxygen ions are imaged as valleys, in spite of the physical topography of the surface, in which the O_b rows are 0.1 nm closer to the tip, as depicted in Figure 2. This is due to the local density of states around each type of atom. The conduction band of the Ti atoms allows for a larger number of unoccupied states for electrons to tunnel into, whereas the oxygen atoms' $2p$ character valence states are very limited. In this case, the electronic configuration plays a larger role than

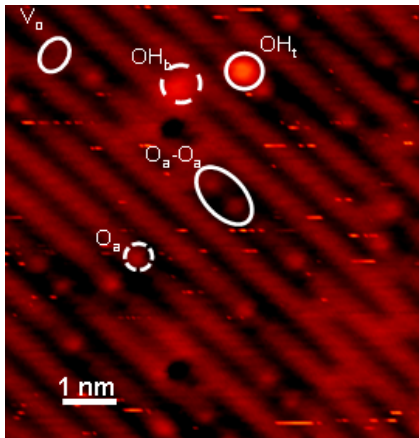


Figure 3: STM image of reduced $\text{TiO}_2(110)$ surface after exposure to 1×10^{-8} Torr of O_2 for 1 min at 300 K. Some of the oxygen vacancies (V_{O}), single oxygen adatoms (O_a) and paired oxygen adatoms ($\text{O}_a - \text{O}_a$) are shown. An example of a bridging hydroxyl (OH_b) and terminal hydroxyl (OH_t) are also marked.

the topographic configuration in the appearance of STM images.¹¹ Bridging oxygen vacancy sites appear as bright spots on the dark oxygen rows, as marked in Figure 3. Oxygen adatoms are revealed as slightly brighter dots on the Ti rows surrounded by a slightly darker region. These features appear both in pairs and singletons depending on the channel of adsorption.^{12,13} Hydroxyl molecules are also sometimes present due to the dissociation of background water molecules on the surface at room temperature.³ Both varieties, the terminal (OH_t) and bridging (OH_b) types are shown so as to differentiate them from adsorbed acetone molecules.

Upon dosing acetone on the oxidized surface, we observed bright protrusions centered on the O_b row, as seen in Figure 4b. We assign these features to be acetone molecules, as supported by density functional theory (DFT) calculations reported by Xia and co-workers.⁹ Figure 4(a)-(b) demonstrates how acetone was observed to preferentially adsorb at vacancy sites. This is contrary to the lack of a temperature programmed desorption (TPD) peak for such a state, reported by Henderson⁵ implying that there is no preference for acetone adsorption at such sites, but in agreement with the recent findings of Xia and co-workers.⁹ We observed the acetone species to be mobile at 300 K. Both diffusion along the row and hopping across rows were observed from sequences of

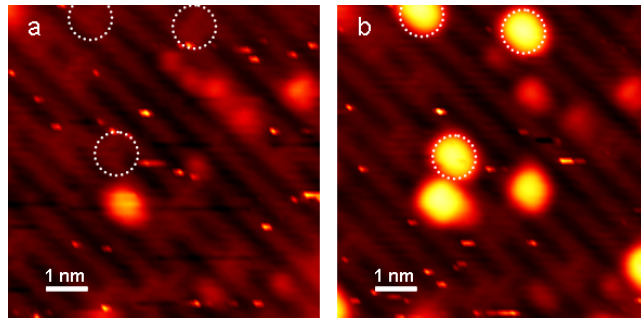


Figure 4: STM image of same area before and after acetone dosing. Dotted circles on left indicate vacancy sites which act as active sites for adsorption of acetone, seen in right image. The bright features prevalent on the right are adsorbed acetone molecules.

isothermal images of the same area for periods of time up to 45 min. Interestingly, when an acetone molecule diffuses along the row past where a O_a is, the O_a is observed to shift as well, by one lattice constant opposite to the motion of the acetone molecule. For every observed diffusion of an O_a , an acetone molecule was observed to diffuse past it. Figure 5(a-c) presents a sequence of images showing one such event. The acetone molecule (green dot) moves along the row, leaving a vacancy behind and causes a shift in the O_a position. From (b)-(c), it then diffuses back, ending in a vacancy near its original position, resulting in a shift of the O_a back to its original position. Water assisted O_a “pseudodiffusion” has been reported previously,¹⁴ but O_a diffusion has never before been observed from acetone, as surface point defects are mostly stationary at 300 K. Analysis of the entire 18 minute movie from which Figure 5 was taken reveals 107 adatoms on the approximately $20 \text{ nm} \times 20 \text{ nm}$ imaged surface. In this area, there were 45 acetone molecules, 20 of which were in motion. There were a relatively high vacancy coverage, with over a hundred V_{O} sites observed with no bonded acetone. Statistically, 9% of the O_a were in motion, and for 70% of those in motion, an acetone molecule was observed to move across the O_a site simultaneously with the O_a diffusion. Xia and co-workers describe two channels for acetone diffusion on rutile $\text{TiO}_2(110)$, as described in the introduction. When acetone diffuses along the O_b row, it leaves its oxygen behind, healing the vacancy it sat on. On the other hand, when acetone diffuses along the Ti_{5c} row, it remains bonded

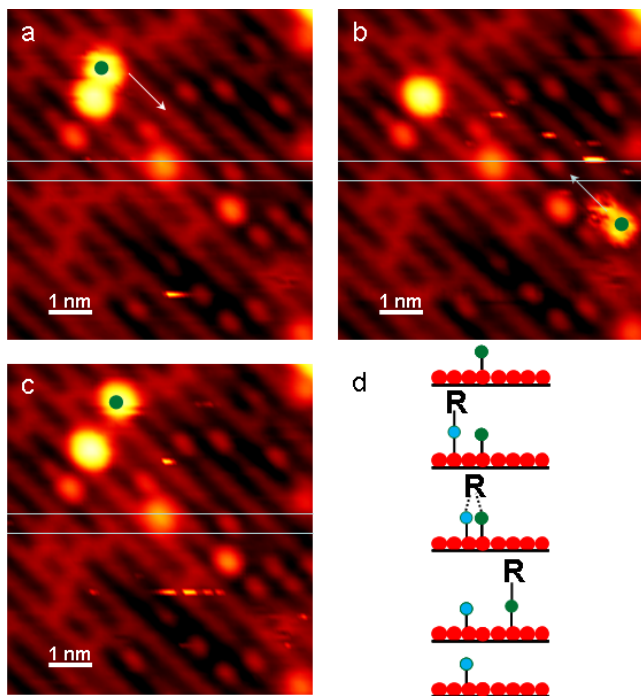


Figure 5: Acetone molecule labeled with the dot diffuses along Ti_{5c} row from (a) to (c). White lines are on same position in all images to show movement. The motion of the adatom by one lattice constant toward the origin of the acetone is easily observable between (a) and (b). When the molecule returns to its initial position in frame (c), the adatom again moves toward where the acetone was. The lower right frame (d) illustrates our proposed method for this diffusion. The red circles are the Ti_{5c} row atoms, the green an O_a , and the blue the oxygen from the acetone.

to an oxygen, leaving a vacancy behind.⁹ As the vacancy is observed to be left behind by the acetone in these O_a diffusion situations, we can infer that the acetone moves along the Ti_{5c} row. We propose a mechanism for acetone assisted O_a diffusion similar to that proposed for H_2O by Du and co-workers.¹⁴ Figure 5d illustrates this mechanism. Acetone binds at Ti^{4+} sites via the lone pair on the oxygen atom becoming a η^1 -acetone species. Acetone can then diffuse on the Ti_{5c} row with a small diffusion barrier ($\sim 0.3eV$ ⁹). When it reaches the O_a they interact, creating a temporary O-C-O bond as an acetone diolate species, which then reverts to a C = O bond on one side. The acetone molecule then continues to diffuse, only now bonded to the oxygen that used to be the O_a , leaving behind its oxygen atom as a new O_a , causing the apparent motion of the O_a on the surface.

Conclusions

We report that acetone molecules preferentially adsorb at V_O sites on oxidized $TiO_2(110)$ surface, despite the lack of a TPD peak for this state reported by other groups.⁵ From here, acetone is free to diffuse at 300 K, demonstrating both along-row and across-row diffusion. Sequences of isothermal STM images from the same area reveal that upon acetone adsorption at room temperature, oxygen adatoms begin to move on the surface. The STM movies directly show a adsorbate-mediated oxygen adatom diffusion mechanism. Acetone diffusing along the Ti_{5c} row reacts with the adsorbed oxygen, bonding to it and continuing to diffuse, leaving its original oxygen behind, one lattice constant from where the O_a was found.

Acknowledgement The author thanks Dr. Tru-ell Hyde, Dr. Lorin Matthews, and everyone at Baylor University and CASPER who worked to make the Research Experience for Undergraduates program the success it is. The author also thanks NSF for funding this research through grant no. PHY-1002637

References

- (1) Diebold, U. *Surface Science Reports* **2003**, 48, 53–229.
- (2) Bak, T.; Nowotny, J.; Sucher, N. J.; Wachsmann, E. *J. Phys. Chem. C* **2011**, 115, 15711–15738.
- (3) Schaub, R.; Lopez, N.; Lægsgaard, E.; Stensgaard, I.; Nørskov, J. K.; Besenbacher, F. *Physical Review Letters* **2001**, 87, 266104.
- (4) Henderson, M. A.; Epling, W. S.; Perkins, C. L.; Peden, C. H. F.; Diebold, U. *J. Phys. Chem. B* **1999**, 103, 5328–5337.
- (5) Henderson, M. A. *J. Phys. Chem. B* **2004**, 108, 18932–18941.
- (6) Wendt, S.; Schaub, R.; Matthiesen, J.; Vestergaard, E.; Wahlström, E.; Rasmussen, M.; Thostrup, P.; Molina, L.; Lægsgaard, E.; Stensgaard, I.; Hammer, B.; Besenbacher, F. *Surface Science* **2005**, 598, 226–245.

- (7) Zhang, Z.; Bondarchuk, O.; Kay, B. D.; White, J. M.; Dohnàlek, Z. *The Journal of Physical Chemistry B* **2006**, *110*, 21840–21845.
- (8) Wendt, S.; Sprunger, P. T.; Lira, E.; Madsen, G. K. H.; Li, Z.; Hansen, J. O.; Matthiesen, J.; Blekinge-Rasmussen, A.; Lægsgaard, E.; Hammer, B. r.; Besenbacher, F. *Science* **2008**, *320*, 1755–1759.
- (9) Xia, Y.; Zhang, B.; Ye, J.; Ge, Q.; Zhang, Z. Unpublished document; Acetone assisted oxygen vacancy diffusion.
- (10) Binnig, G.; Rohrer, H. *Surface Science* **1983**, *126*, 236–244.
- (11) Diebold, U.; Anderson, J. F.; Ng, K.-O.; Vanderbilt, D. *Physical Review Letters* **1996**, *77*, 1322–1325.
- (12) Tan, S.; Ji, Y.; Zhao, Y.; Zhao, A.; Wang, B.; Yang, J.; Hou, J. *J. Am. Chem. Soc.* **2011**, *133*, 2002–2009.
- (13) Du, Y.; Deskins, N. A.; Zhang, Z.; Dohnàlek, Z.; Dupuis, M.; Lyubinetsky, I. *Physical Chemistry Chemical Physics* **2010**, *12*, 6337.
- (14) Du, Y.; Deskins, N. A.; Zhang, Z.; Dohnàlek, Z.; Dupuis, M.; Lyubinetsky, I. *Physical Review Letters* **2009**, *102*, 096102.